iScience

CellPress

Article

Nuclear Factor-kappaB Gates $Na_v1.7$ Channels in DRG Neurons via Protein-Protein Interaction

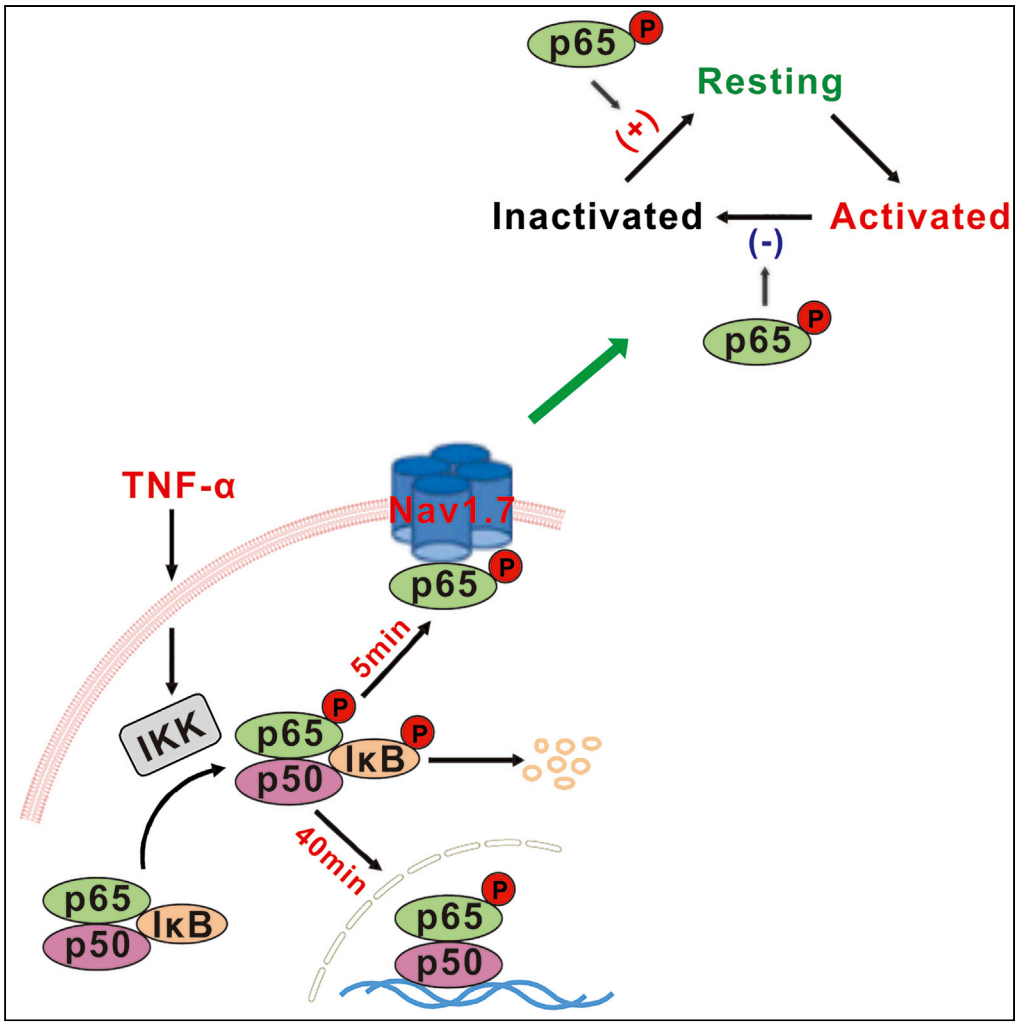

Man-Xiu Xie, Xiao-Long Zhang, Jing Xu, ..., Rui-Ping Pang, Ke Ma, Xian-Guo Liu

marke72@163.com (K.M.)
liuxg@mail.sysu.edu.cn (X.-G.L.)

HIGHLIGHTS

NF-κB *p*-p65 interacts with $Na_v1.7$ in the membrane of DRG neurons

The interaction is reversible, depending on the cytoplasmic *p*-p65 content

Reducing cytoplasmic *p*-p65 rapidly attenuates the interaction and $Na_v1.7$ currents

The rapid effect on $Na_v1.7$ channels is independent of *p*-p65 nuclear translocation

Xie et al., iScience *19*, 623–633
September 27, 2019
https://doi.org/10.1016/j.isci.2019.08.017

iScience

CellPress

Article

Nuclear Factor-kappaB Gates $Na_v1.7$ Channels in DRG Neurons via Protein-Protein Interaction

Man-Xiu Xie,[1,6] Xiao-Long Zhang,[5,6] Jing Xu,[2,6] Wei-An Zeng,[1] Dai Li,[2] Ting Xu,[2] Rui-Ping Pang,[2] Ke Ma,[3,*] and Xian-Guo Liu[2,3,4,7,*]

SUMMARY

It is well known that nuclear factor-kappaB (NF-κB) regulates neuronal structures and functions by nuclear transcription. Here, we showed that phospho-p65 (*p*-p65), an active form of NF-κB subunit, reversibly interacted with $Na_v1.7$ channels in the membrane of dorsal root ganglion (DRG) neurons of rats. The interaction increased $Na_v1.7$ currents by slowing inactivation of $Na_v1.7$ channels and facilitating their recovery from inactivation, which may increase the resting state of the channels ready for activation. In cultured DRG neurons TNF-α upregulated the membrane *p*-p65 and enhanced $Na_v1.7$ currents within 5 min but did not affect nuclear NF-κB within 40 min. This non-transcriptional effect on $Na_v1.7$ may underlie a rapid regulation of the sensibility of the somatosensory system. Both NF-κB and $Na_v1.7$ channels are critically implicated in many physiological functions and diseases. Our finding may shed new light on the investigation into the underlying mechanisms.

INTRODUCTION

Nuclear factor-kappaB (NF-κB), a potent transcription factor, is highly conserved from insect to human and plays critical roles in a wide variety of physiological and pathological processes, such as memory storage (Meffert and Baltimore, 2005), immunity and cancer (Taniguchi and Karin, 2018), neurodegenerative diseases (Srinivasan and Lahiri, 2015), and chronic pain (Niederberger and Geisslinger, 2008). NF-κB p50/p65/inhibitor of NF-κB (IκB-α) complex is located in the cytoplasm. On activation, both p65 and IκB-α are phosphorylated, and then *p*-IκB-α is degenerated after ubiquitination, whereas phospho-p65 (*p*-p65) is translocated into the nucleus, where it regulates gene transcription (Niederberger and Geisslinger, 2008). At present, all the functions of NF-κB are attributed to the transcriptional effect in vertebrate (Salles et al., 2014). There are two NF-κB activation pathways, classical and alternative; tumor necrosis factor alpha (TNF-α) is critical in both of them (Wajant and Scheurich, 2011).

Dorsal root ganglion (DRG) neurons play an essential role in detecting the changes in the external environment. As a pseudounipolar neuron, its peripheral axon branches transfer different forms of sensory stimuli into action potentials (APs) and its central axon branches conduct the APs to spinal dorsal horn (Chahine and O'Leary, 2014). Activation of voltage-gated sodium (Na_v) channels is indispensable for the initiation and conduction of APs. Among the nine subunits of Na_v channels (Catterall et al., 2005), tetrodotoxin-sensitive (TTX-S) channels $Na_v1.3$, $Na_v1.6$, and $Na_v1.7$ and TTX-resistant (TTX-R) channels $Na_v1.8$ and $Na_v1.9$ are proved important for the excitability of DRG neurons (Dib-Hajj et al., 2010). Previous works show that activation of TNF-α/NF-κB signaling leads to chronic hyperexcitability of DRG neurons (He et al., 2010; Huang et al., 2014; Tamura et al., 2014; Zang et al., 2010) and of cortical neurons (Chen et al., 2015) by transcriptional upregulation of sodium channels. In the present work, we provided evidence that *p*-p65 also enhances Na^+ currents in a transcription-independent way. The data uncover a novel mechanism by which TNF-α/NF-κB signaling rapidly regulates cell excitability.

RESULTS

p-p65 (s311) Is Located in the Membrane of DRG Neurons, and Reducing Cytoplasmic *p*-p65 Inhibits Na^+ Currents within Minutes

Immunofluorescent staining showed that *p*-p65 (s311) was located not only in the nucleus but also in the membrane of DRG neurons in both naive and neuropathic rats, namely, vincristine (VCR, a chemotherapeutic agent)-induced peripheral neuropathy or lumbar 5 spinal nerve ligation (L5-SNL) (Figures 1A–1C). Western blots

[1]Department of Anesthesiology, Sun Yat-sen University Cancer Center, State Key Laboratory of Oncology in South China, Collaborative Innovation Center for Cancer Medicine, 651 Dongfeng East Road, Guangzhou 510060, China

[2]Pain Research Center and Department of Physiology, Zhongshan School of Medicine of Sun Yat-sen University, 74 Zhongshan Road 2, Guangzhou 510080, China

[3]Department of Pain Management, Xinhua Hospital, Shanghai Jiaotong University School of Medicine, Shanghai 91603, China

[4]Guangdong Provincial Key Laboratory of Brain Function and Disease, 74 Zhongshan Road 2, Guangzhou 510080, China

[5]Medical Research Center of Guangdong Provincial People's Hospital, Guangdong Academy of Medical Sciences, 106 Zhongshan Road 2, Guangzhou 510080, China

[6]These authors contributed equally

[7]Lead Contact

*Correspondence: marke72@163.com (K.M.), liuxg@mail.sysu.edu.cn (X.-G.L.)

https://doi.org/10.1016/j.isci.2019.08.017

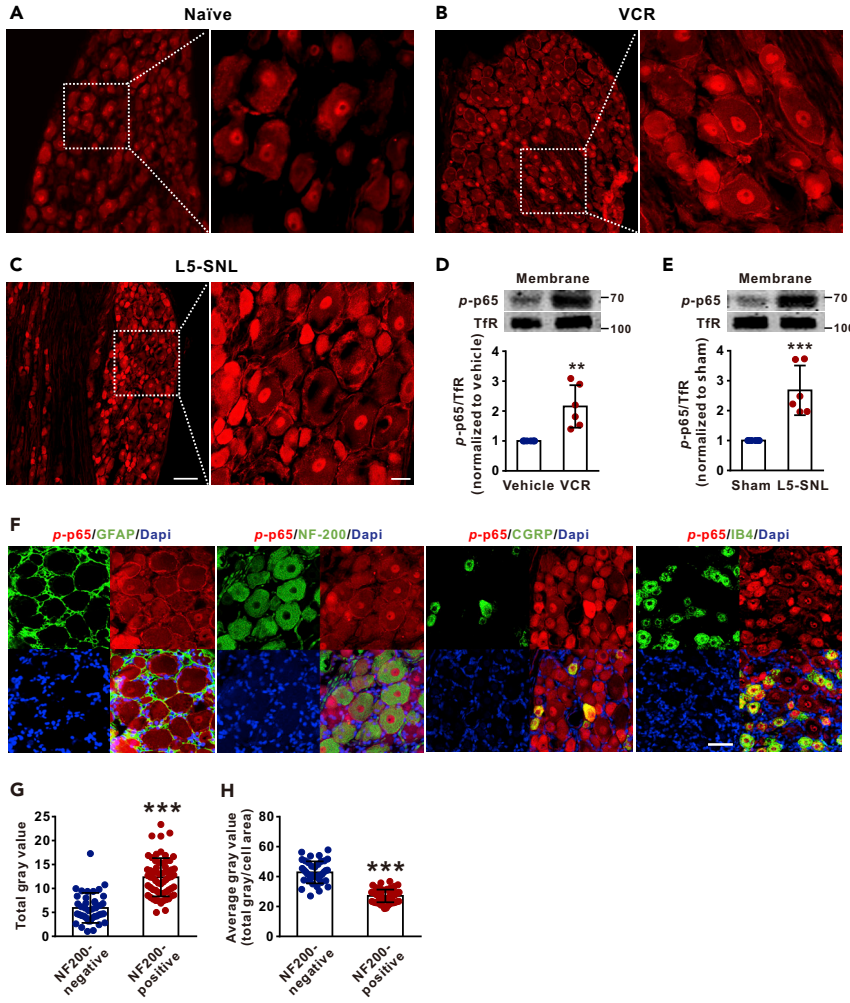

Figure 1. Phospho-p65 (s311) Is Located in the Membrane of Dorsal Root Ganglion Neurons and Is Increased in Neuropathic Conditions

(A–C) The representative confocal images show that *p*-p65 is located not only in the nucleus but also in the membrane of DRG neurons in naive (A), vincristine (VCR)-treated (B) and L5-spinal nerve ligation (L5-SNL) (C) rats. Scale bars: left 100 μm, right 20 μm.

(D and E) The western blots show that *p*-p65 in membrane is increased in VCR-treated (D) and L5-SNL (E) rats, compared with vehicle and sham rats. Samples were harvested after the last VCR injection or 10 days after L5-SNL. n = 6 in each group. **p < 0.01, ***p < 0.001 compared with vehicle or sham group.

(F) The cell types that express *p*-p65 (s311) in DRG neurons. Scale bars: 50 μm.

(G and H) The total (G) and the average (H) gray value of *p*-p65 signal in NF-200 positive (larger-diameter) and NF-200-negative (small-diameter) neurons. n = 40 in NF200-negative group, n = 62 in NF200-positive group. ***p < 0.001 compared with the corresponding NF200-negative group. Two-tailed t test. The specificity of the antibody for *p*-p65 (s311) was identified in Figure S2A. Data expressed as mean ± SD. The control of membrane fractionation process was shown in Figure S2C.

with membrane protein extract of DRGs revealed that the membrane *p*-p65 level was significantly higher in either VCR-treated or L5-SNL rats compared with vehicle-treated or sham-operated rats (Figures 1D and 1E). Double staining showed that *p*-p65 (s311) was colocalized with the markers of large neurons (NF-200) and of small neurons (CGRP and IB4) but not with the marker of satellite glial cells (GFAP) (Figure 1F). We quantified the levels of *p*-p65 in large (NF-200 positive) and small (NF-200 negative) DRG neurons. As shown in Figures 1G and 1H, the total gray value of *p*-p65 signal in large neurons was higher than that in small neurons, but the average gray value of *p*-p65 signal (total gray value/cell area) in large neurons was lower than that in small neurons. The data indicate that *p*-p65 is expressed in all types of DRG neurons, although expression is more intensive in small ones. Therefore, in the following experiments all sizes of DRG neurons were used.

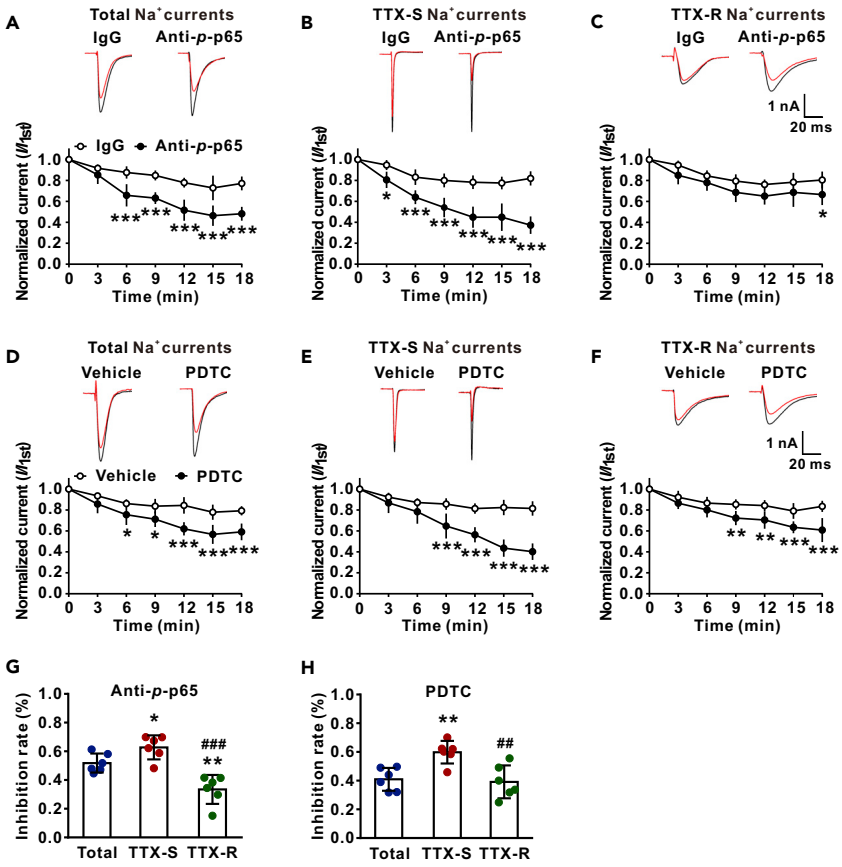

Figure 2. Intracellular Application of Anti-*p*-p65 (s311) or Extracellular Application of PDTC Preferably Reduces TTX-S Na^+ Currents over TTX-R Ones within Minutes

(A–C) The effects of intracellular anti-*p*-p65 (10 μg/mL) on total (A), TTX-S (B) and TTX-R (C) Na^+ currents. The raw traces were recorded immediately on onset (black) and 18 min (red) after recordings. n = 6 in each group. *p < 0.05, ***p < 0.001 compared with the corresponding IgG group. (D–F) The effects of extracellular NF-κB inhibitor PDTC (10 nM) on total (D), TTX-S (E) and TTX-R (F) Na^+ currents. The raw traces were recorded immediately on onset (black) and 18 min (red) after recordings. n = 6 in each group. *p < 0.05, **p < 0.01, ***p < 0.001 compared with the corresponding vehicle group.

(G and H) The histograms show the inhibitory rates of anti-*p*-p65 (G) and PDTC (H) on total, TTX-S, and TTX-R currents at 18 min after recordings. *p < 0.05, **p < 0.01 compared with total currents; $^{\#\#}$p < 0.01, $^{\#\#\#}$p < 0.001 compared with TTX-S currents. A-F, two-way repeated measures ANOVA followed by Bonferroni's multiple comparisons test; G and H, one-way ANOVA followed by Holm-Sidak's multiple comparisons test. Data expressed as mean ± SD.

The primary function of DRG neurons is production of APs in response to various sensory stimuli, and opening of Na_v channels is critical in this process. We, therefore, tested if membrane *p*-p65 might regulate the Na_v channels. To do this, total Na^+, TTX-S, or TTX-R currents were recorded in the DRG neurons of VCR-treated rats with microelectrodes containing *p*-p65 antibody (10 μg/mL) or IgG. TTX-S and TTX-R currents were isolated by blocking TTX-R channels with A-803467 (1 μM) (Jarvis et al., 2007) (Figure S1) and by blocking TTX-S channels with TTX (300 nM), respectively. As shown in Figures 2A–2C, compared with IgG control group, a significant reduction of total Na^+, TTX-S, or TTX-R currents was evident at 6, 3, and 18 min after the onset of recordings. The results indicate that *p*-p65 facilitates Na_v currents. To confirm this, pyrrolidinedithiocarbamate (PDTC, 10 nM), an NF-κB inhibitor that reduces intracellular *p*-p65 by inhibition of IκB-ubiquitin ligase activity (Hayakawa et al., 2003), was applied extracellularly 1 min after recordings. We found that PDTC inhibited total Na^+ currents, TTX-S currents, or TTX-R currents within 6–9 min, compared with the vehicle group (Figures 2D–2F). We found that both intracellular anti-*p*-p65 and extracellular PDTC preferably inhibited TTX-S currents over TTX-R ones (Figures 2G and 2H).

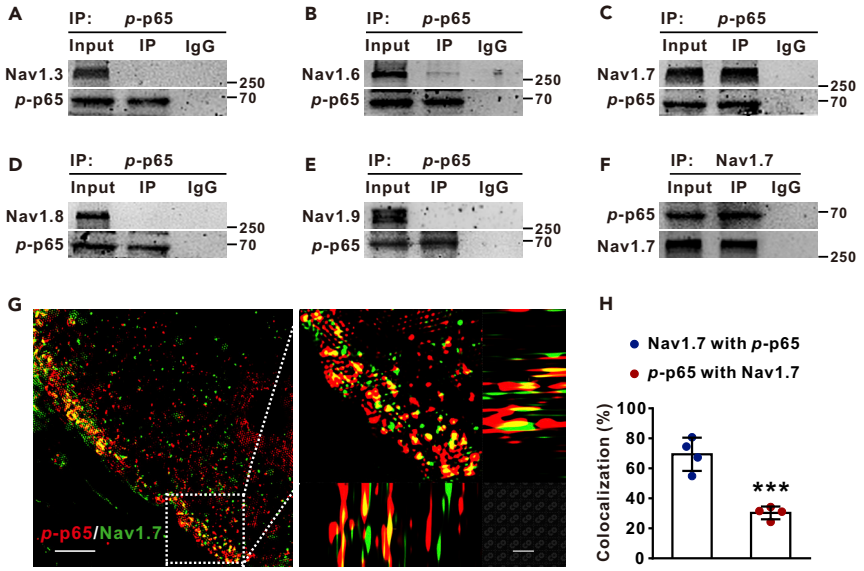

Figure 3. *p*-p65 (s311) Interacts with $Na_v1.7$ Channels in the Membrane of DRG Neurons

(A–F) Co-IP with DRG protein extract of VCR-treated rats shows that *p*-p65 strongly interacted with $Na_v1.7$ (C and F), weakly with $Na_v1.6$ (B), but not with $Na_v1.3$ (A), $Na_v1.8$ (D), or $Na_v1.9$ (E).

(G) The structured illumination microscopies show that *p*-p65 is colocalized with $Na_v1.7$ in DRG neuron membrane of VCR rat. Scale bars: left 10 μm, right 5 μm.

(H) Quantification data show colocalization rates of $Na_v1.7$ with *p*-p65 (colocalized yellow spots/total $Na_v1.7$ positive spots) and those of *p*-p65 with $Na_v1.7$ (colocalized yellow spots/total *p*-p65 positive spots) in membrane. n = 4 in each group. ***$p < 0.001$ compared with $Na_v1.7$ with *p*-p65 group. The specificity of the antibody for $Na_v1.7$ was identified (Figure S2B). Two-tailed t test. Data expressed as mean ± SD.

Membrane *p*-p65 Gates $Na_v1.7$ Channels by Protein-Protein Interaction

Our data that *p*-p65 was located in the membrane and that PDTC inhibited Na_v currents within minutes suggested that *p*-p65 might regulate Na_v channels, non-transcriptionally. To investigate the mechanisms underlying the rapid effect, we tested the possibility that *p*-p65 may gate sodium channels by protein-protein interaction. The co-immunoprecipitation (Co-IP) experiments with the protein extract of DRGs from VCR-treated rats showed that *p*-p65 interacted potently with $Na_v1.7$, weakly with $Na_v1.6$, and barely with $Na_v1.3$, $Na_v1.8$, or $Na_v1.9$ (Figures 3A–3F). To confirm the *p*-p65-$Na_v1.7$ interaction, we performed high-resolution images of structured illumination microscopy and found that 69.4 ± 11.1% of $Na_v1.7$ was colocalized with *p*-p65, whereas only 30.3 ± 4.3% of *p*-p65 was colocalized with $Na_v1.7$ in membrane of DRG neurons from VCR-treated rats (Figures 3G and 3H).

We then investigated the effect of the interaction on TTX-S $Na_v1.7$ channels. If *p*-p65 was required for activation of $Na_v1.7$ channels, blockade of $Na_v1.7$ would occlude the inhibitory effect of PDTC on TTX-S currents as shown in Figures 2D–2F. Indeed, we found that PDTC (10 nM) failed to affect TTX-S currents when applied 15 min after extracellular application of ProTxII (5 nM), a selective $Na_v1.7$ blocker (Schmalhofer et al., 2008), in DRG neurons of VCR-treated rats (Figures 4A and 4B). Conversely, ProTxII also failed to affect TTX-S Na^+ currents when applied 15 min after PDTC (Figures 4C and 4D). To further study the effect of *p*-p65 on $Na_v1.7$ channels, we repeated the experiments with ICA-121431 (5 μM), a potent rat $Na_v1.7$ channel blocker (IC_{50}: 37 nM) (McCormack et al., 2013), and found that the effects of ICA-121431 and PDTC on TTX-S currents were also occluded by each other (Figures 4E–4H). In addition, we found that intracellular application of anti-*p*-p65 also blocked the inhibitory effect of ProTxII on TTX-S currents (Figures 4I and 4J). The mutual inhibition between PDTC and $Na_v1.7$ blockers on TTX-S currents was also observed in the DRG neurons from naive rats (Figures 5A–5H).

To investigate how reducing intracellular *p*-p65 decreases $Na_v1.7$ currents, we measured *p*-p65 and $Na_v1.7$ in DRG membrane from VCR- and vehicle-treated rats. The western blots with membrane protein extract of DRGs revealed that both *p*-p65 and $Na_v1.7$ were significantly increased in the VCR-treated group

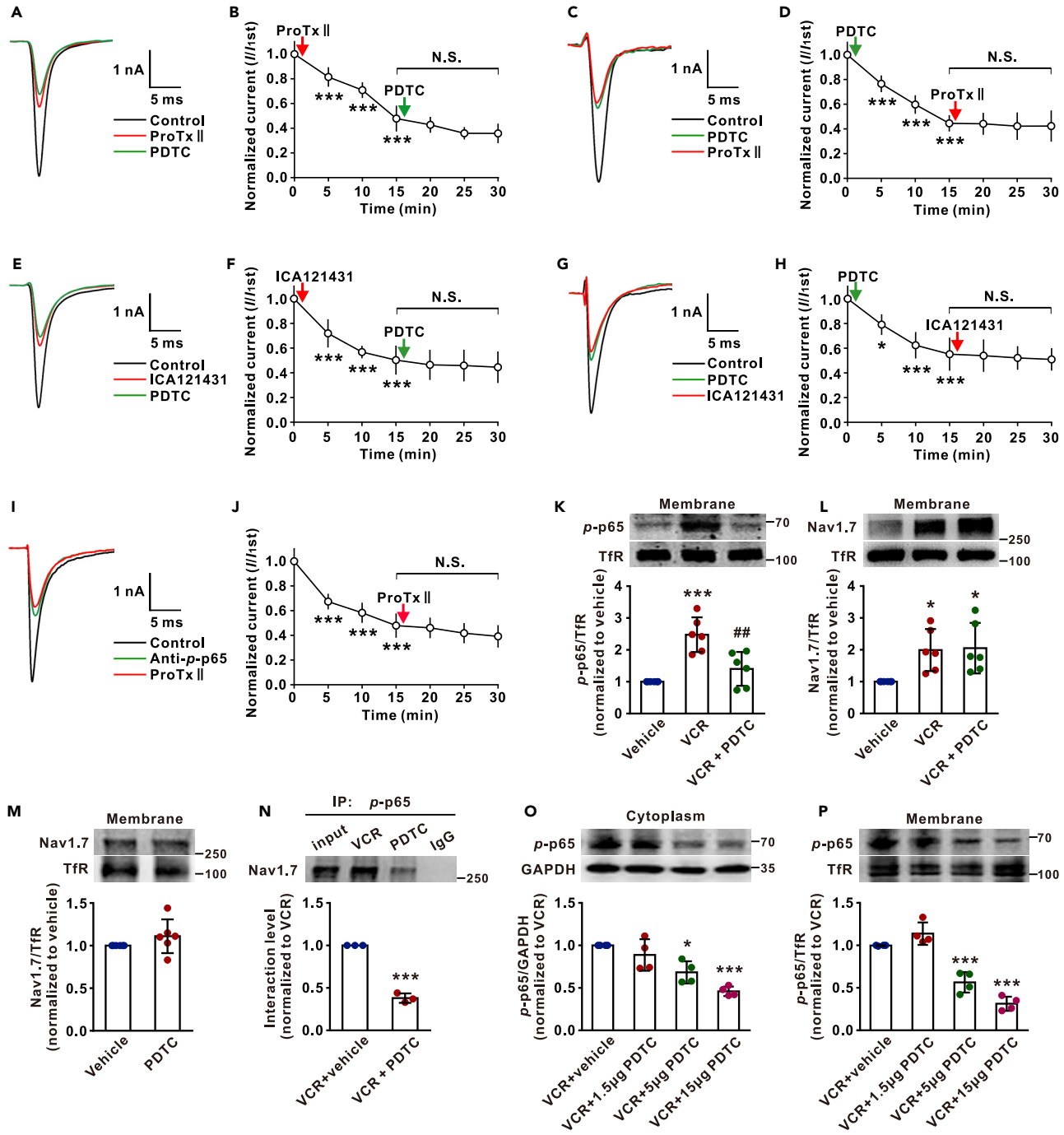

Figure 4. NF-κB Inhibitor PDTC Inhibits $Na_v1.7$ Channels by Reducing $Na_v1.7$- *p*-p65 Interaction in Membrane of DRG Neurons

(A) The traces show TTX-S currents recorded in indicated conditions.

(B) ProTxII (5 nM) occludes the effect of PDTC (10 nM) on TTX-S currents of VCR rats. n = 7. ***p < 0.001 compared with predrug control.

(C) The traces show TTX-S currents recorded in indicated conditions.

(D) PDTC (10 nM) occludes the effect of ProTxII (5 nM) on TTX-S currents of VCR rats. n = 6. ***p < 0.001 compared with predrug control.

(E) The traces show TTX-S currents recorded in indicated conditions.

(F) ICA121431 (5 μM) occludes the effect of PDTC on TTX-S currents of VCR rats. n = 6. ***p < 0.001 compared with predrug control.

(G) The traces show TTX-S currents recorded in indicated conditions.

(H) PDTC occludes the effect of ICA121431 on TTX-S currents of VCR rats. n = 6. *p < 0.05, ***p < 0.001 compared with predrug control.

Figure 4. *Continued*

(I) The traces show TTX-S currents recorded in indicated conditions.

(J) Intracellular application of anti-*p*-p65 blocks the effect of ProTxII on TTX-S currents of VCR rats. n = 6. ***p < 0.001 compared with the first recording.

(K and L) Thirty minutes after intrathecal injection of PDTC (15 μg/10 μL), both *p*-p65 (K) and $Na_v1.7$ (L) in the membrane were tested. n = 6 in each group. *p < 0.05, ***p < 0.001 compared with vehicle group; $^{\#\#}$p < 0.01 compared with VCR group.

(M) The membrane $Na_v1.7$ in DRGs of naive rats was measured 30 min after intrathecal injection of PDTC (15 μg/10 μL). n = 6 in each group.

(N) The interaction between *p*-p65 and $Na_v1.7$ in DRGs of VCR-treated rats was reduced 30 min after intrathecal injection of PDTC (15 μg/10 μL). $Na_v1.7$ was immunoprecipitated by *p*-p65 antibody. n = 3 in each group. ***p < 0.001 compared with VCR + vehicle group.

(O and P) Intrathecal injection of PDTC (10 μL) dose-dependently reduced *p*-p65 levels in both membrane (P) and cytoplasm (O). The DRG tissues were harvested 30 min after injection. n = 4 in each group. *p < 0.05, ***p < 0.001 compared with VCR + vehicle group. B, D, F, H, J, K, L, O, P, one-way ANOVA followed by Tukey's multiple comparisons test. M, N, Two-tailed t test. Data expressed as mean ± SD. N.S. mean not significant.

compared with the vehicle-treated group. Importantly, intrathecal injection of PDTC reduced *p*-p65 but did not affect $Na_v1.7$ in cell membrane within 30 min (Figures 4K and 4L). The results indicate that the inhibitory effect of extracellular PDTC or intracellular anti-*p*-p65 on Na^+ currents is due to the reduction of *p*-p65 but not of $Na_v1.7$ in cell membrane. We found that PDTC also did not affect membrane $Na_v1.7$ in DRGs of naive rats (Figure 4M). Our data that PDTC rapidly reduces TTX-S Na^+ currents and membrane *p*-p65 suggested that the interaction between *p*-p65 and $Na_v1.7$ in membrane might be reversible, depending on its intracellular content. To test this, we performed Co-IP with DRGs from VCR-treated rats and found that the *p*-p65-$Na_v1.7$ interaction was substantially reduced 30 min after intrathecal injection of PDTC (Figure 4N). Consistently, intrathecal injection of PDTC reduced *p*-p65 in both cytoplasm and membrane dose-dependently (Figures 4O and 4P). The data indicate that *p*-p65 may regulate $Na_v1.7$ channels by reversible interaction with the channel subtype.

TNF-α Enhances Membrane *p*-p65 (s311) and $Na_v1.7$ Currents within Minutes in Cultured DRG Neurons

To test if nuclear transcription may also contribute to the rapid effect of *p*-p65 on $Na_v1.7$ channels, we performed the experiments with cultured DRG neurons. As TNF-α plays a key role in both classical and alternative NF-κB activation pathways (Wajant and Scheurich, 2011), we incubated DRG neurons from naive rats with rat recombinant TNF-α (rrTNF-α, 100 ng/mL) and measured *p*-p65 levels in membrane and in nuclei at different time points afterward. A significant increase of *p*-p65 was detected in membrane within 5 min (Figure 6A), whereas in nuclei at 120 min but not within 40 min (Figures 6B and 6C). That is, in response to TNF-α stimulation, *p*-p65 membrane translocation is at least 40 min earlier than its nuclear translocation. Furthermore, we found that rrTNF-α did not affect membrane $Na_v1.7$ level within 20 min (Figure 6D) but enhanced $Na_v1.7$ currents, isolated by subtraction of the ProTxII-resistant Na^+ currents from total Na^+ currents (Li et al., 2018), within 5 min. The I-V curves (Figure 6E) showed that the peak $Na_v1.7$ currents in the DRG neurons treated with rrTNF-α (100 ng/mL for 5 min) were significantly higher, compared with the neurons treated with the vehicle. To test if the effect of rrTNF-α on $Na_v1.7$ currents is mediated by membrane *p*-p65, DRG neurons were incubated with rrTNF-α for 5 min and then with PDTC (10 nM) for 15 min. The peak currents in the rrTNF-α + PDTC group were significantly lower compared with the rrTNF-α alone group and were not different from the vehicle group (Figure 6E). Therefore, the rapid effect of TNF-α on $Na_v1.7$ channels results from the *p*-p65-$Na_v1.7$ interaction and is independent of *p*-p65 nuclear transcription and the membrane $Na_v1.7$ level. To investigate the potential mechanism by which *p*-p65 regulates $Na_v1.7$ currents, we performed experiments with HEK293 cells that express $Na_v1.7$. The results showed that PDTC accelerated inactivation and delayed recovery but did not affect activation of $Na_v1.7$ channels (Figures 6F–6H and Table 1). In consistence with the electrophysiological data, we found that intrathecal injection of PDTC alleviated the decrease in mechanical pain thresholds induced by VCR within 30 min (Figure 6I).

DISCUSSION

As mentioned in the Introduction section, NF-κB plays important roles in many physiological and pathological processes. Up to date, all the functions of NF-κB are explained by its transcriptional effect. In this present work, we showed for the first time that *p*-p65 was also located in the membrane of DRG neurons and was increased in neuropathic conditions *in vivo* or in response to TNF-α stimulation in cultured DRG neurons. The membrane *p*-p65 regulated $Na_v1.7$ channels by protein-protein interaction. In membrane of DRG neurons, ~70% of $Na_v1.7$ was colocalized with *p*-p65, whereas only ~30% of *p*-p65 is colocalized with $Na_v1.7$ (Figure 3H). The data suggested that *p*-p65 might also regulate cell function by interacting with

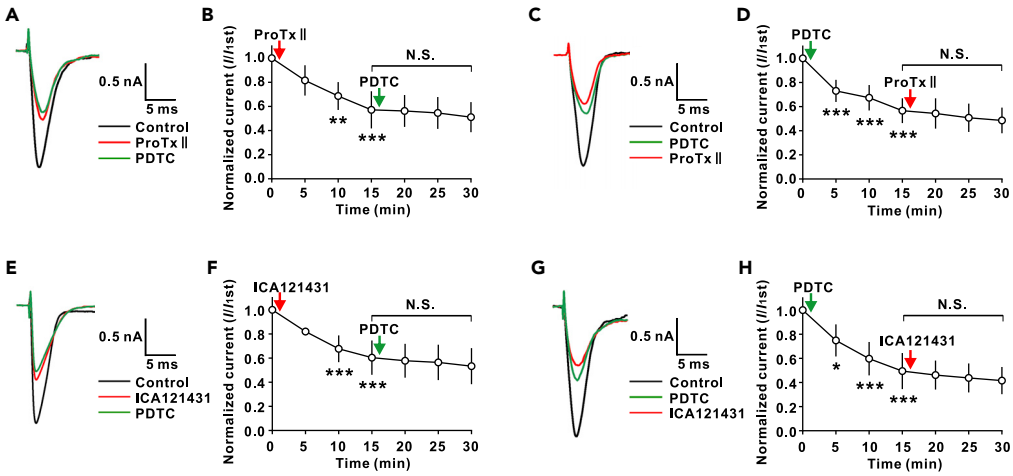

Figure 5. The Effects of PDTC and $Na_v1.7$ Blockers on TTX-S Channels Occlude Each Other in DRG Neurons of Naive Rats

(A) The traces show TTX-S currents recorded in indicated conditions.

(B) ProTxII blocks the effect of PDTC on TTX-S currents. n = 6. **p < 0.01, ***p < 0.001 compared with predrug control.

(C) The traces show TTX-S currents recorded in indicated conditions.

(D) PDTC blocks the effect of ProTxII on TTX-S currents. n = 6. ***p < 0.001 compared with predrug control.

(E) The traces show TTX-S currents recorded in indicated conditions.

(F) ICA-121431 occludes the effect of PDTC on TTX-S currents. n = 6. ***p < 0.001 compared with predrug control.

(G) The traces show TTX-S currents recorded in indicated conditions.

(H) PDTC blocks the effect of ICA-121431 on TTX-S currents. n = 6. *p < 0.05, ***p < 0.001 compared with predrug control.

B, D, F, H, one-way ANOVA followed by Tukey's multiple comparisons test. Data expressed as mean ± SD. N.S. mean not significant.

other proteins in cell membranes. Further studies are needed to elucidate this issue. We also found that reduction of cytoplasmic *p*-p65 by intracellular anti-*p*-p65 or extracellular PDTC also inhibited TTX-R currents. As no interaction between *p*-p65 and TTX-R channels ($Na_v1.8$ and $Na_v1.9$) in DRG neurons was detected, the mechanisms underlying the effect remains elusive.

On activation, Na_v channels go through rapid transitions from the resting to opening, inactivated state and eventually recover to the resting state (Aldrich et al., 1983). $Na_v1.7$ is distinguished from other TTX-S channels by slow closed-state inactivation, which is suggested to determine action potential threshold by permitting to pass a current in response to small slow depolarization (see Dib-Hajj et al., [2007] for a review). Our data showed that PDTC reduced $Na_v1.7$-*p*-p65 interaction (Figure 4N) and accelerated inactivation and delayed recovery but did not affect activation of $Na_v1.7$ channels (Figures 6F–6H and Table 1). That is, *p*-p65-$Na_v1.7$ interaction may increase $Na_v1.7$ currents by slowing inactivation and facilitating recovery from inactivation, leading to an increase of the resting state of $Na_v1.7$ that is ready for opening.

Previous works show that NF-κB is expressed at the synapses and neuromuscular junction and in neuronal fibers, and the local NF-κB is also believed to regulate gene expression (Dresselhaus et al., 2018; Meffert and Baltimore, 2005; Salles et al., 2014). The synaptic NF-κB is also speculated to function locally. Up to date, however, no direct evidence is available in vertebrate (Salles et al., 2014). In drosophila, it has been shown that Dorsal (homolog of NF-κB) in neuromuscular junction regulates glutamate receptor density in a transcription-independent way (Heckscher et al., 2007).

$Na_v1.7$ has been intensively studied in the sensory system. In human, loss of function of $Na_v1.7$ leads to complete inability to sense pain (Cox et al., 2006) and odors (Weiss et al., 2011), whereas gain of its function results in paroxysmal extreme pain disorder (Fertleman et al., 2006). In rodents, deletion of $Na_v1.7$ in mouse DRG neurons attenuates acute nociception and nerve injury-, inflammation- and burn injury-induced pain hypersensitivity (Minett et al., 2012, 2014; Nassar et al., 2004; Shields et al., 2012). Blockage of $Na_v1.7$ significantly alleviates neuropathic pain induced by the chemotherapeutic drug paclitaxel (Li et al., 2018). A recent study shows that mutation of $Na_v1.7$ in human patients leads to functional absence of nociceptors (McDermott et al., 2019). Accordingly, $Na_v1.7$ is a prominent target for treating chronic pain. Our finding that *p*-p65 gates $Na_v1.7$

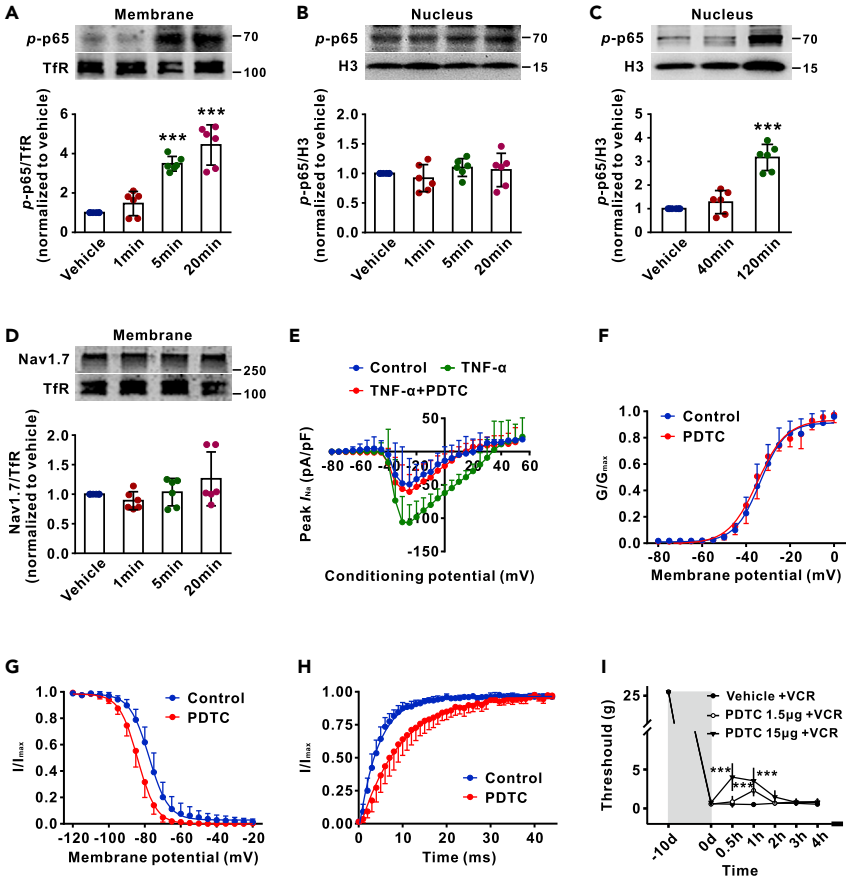

Figure 6. TNF-α Enhances Membrane *p*-p65 (s311) and $Na_v1.7$ Currents in Cultured DRG Neurons without Affecting Nuclear *p*-p65 and Membrane $Na_v1.7$ within Minutes

(A–D) The western blots show the levels of *p*-p65 and $Na_v1.7$ in membrane (A and D) or nucleus (B and C) of DRG neurons at indicated time points after application of rrTNF-α (100 ng/mL). n = 6 in each group. ***p < 0.001 compared with vehicle group.

(E) The I-V curves show the peak $Na_v1.7$ currents recorded under different potentials in indicated groups. n = 9, 8, and 9 in control, TNF-α, and TNF-α + PDTC group.

(F–H) The effects of PDTC (10 nM) on activation (F), inactivation (G), and recovery (H) of $Na_v1.7$ channels in HEK293 cells. n = 6–7 in each group.

(I) Intrathecal injection of NF-κB inhibitor PDTC (10 μL) reduces mechanical allodynia in vincristine (VCR)-treated rats within 30 min. n = 5 in each group. ***p < 0.001 compared with vehicle + VCR group. The data in A, B, C, D, and E were analyzed with one-way ANOVA followed by Tukey's multiple comparisons test, and in F, G, and H with two-tailed t test. I, two-way repeated measures ANOVA followed by Bonferroni's multiple comparisons test. Data expressed as mean ± SD. The control of nuclear fractionation process was shown in Figure S2C.

channels in naive and neuropathic rats raises a possibility that selective blockage of the interaction between *p*-p65 and $Na_v1.7$ channels may treat the chronic pain resulting from gain of $Na_v1.7$ function. The new strategy can avoid the side effects of NF-κB inhibitor owing to its transcriptional inhibition.

In addition, global deletion of $Na_v1.7$ in mice leads to death shortly after birth (Nassar et al., 2004), indicating that the channel subtype should play important roles in other vital systems. Consistently, $Na_v1.7$ is found in the brain regions that regulate autonomic and endocrine systems of rats (Morinville et al., 2007) and in airway parasympathetic ganglia of mice, guinea pig, and human (Kocmalova et al., 2017). Furthermore, $Na_v1.7$ is also expressed in human immature dendritic cells (Zsiros et al., 2009). $Na_v1.7$ expressed in gastric cancer cells and human non-small cell lung cancer cells promotes cancer progression or invasion (Campbell et al., 2013; Xia et al., 2016). It is interesting to know if NF-κB also non-transcriptionally regulates the $Na_v1.7$ in these cells.

	Activation		Inactivation		Recovery
	$V_{0.5}$	k	$V_{0.5}$	k	τ
Control	−33.6 ± 3.4	5.7 ± 1.7	−77.6 ± 2.5	5.4 ± 0.2	4.5 ± 0.8
PDTC	−34.8 ± 3.6	6.6 ± 1.0	−84.0 ± 2.3[a]	5.1 ± 0.4	9.2 ± 3.3[b]

Table 1. The Effects of PDTC on the Parameters of Activation, Inactivation, and Recovery of $Na_v1.7$ Channels in HEK293 Cells

Mean values were derived from Boltzmann equation fits of individual data sets as described in the Methods.

[a]$p < 0.001$ vs. corresponding control. Two-tailed paired student *t* test. Data expressed as mean ± SD.

[b]$p < 0.01$

It has been well established that TNF-α produces a persistent hyperexcitability through gene transcription in DRG (He et al., 2010; Huang et al., 2014; Tamura et al., 2014; Zang et al., 2010) and in cortical neurons (Chen et al., 2015). TNF-α has also been repeatedly demonstrated to induce an acute excitation of DRG neurons (Liu et al., 2002; Zhang et al., 2002) and of subfornical organ neurons (Simpson and Ferguson, 2017). TNF-α enhances sodium currents in DRG neurons within minutes (Jin and Gereau, 2006). The mechanism underlying the rapid effect is unknown. Our result that *p*-p65 regulates $Na_v1.7$ channels by protein-protein interaction may explain the TNF-α-induced acute excitation. A previous work shows that NF-κB in DRG neurons is activated by noxious electrical, chemical, and thermal stimulation of peripheral tissues within minutes, and the physiological significance of this rapid NF-κB activation is not clarified (Fujikawa et al., 2011). We propose that NF-κB may rapidly regulate somatosensory function via gating of ion channels in DRG neurons.

Together, activation of TNF-α/NF-κB signaling induces not only the chronic hypersensitivity of DRG neurons by nuclear transcription but also an acute excitation of the neurons by protein-protein interaction. In this process, NF-κB functions not only as a transcription factor but also as an ion channel modulator. Our finding may open up a new arena for investigating mechanisms by which NF-κB regulates cell functions.

Limitations of the Study

We explored that *p*-p65 rapidly regulates $Na_v1.7$ by protein-protein interaction in DRG neurons, whereas the mechanism underlying the interaction was not investigated. NF-κB is also highly expressed in the neurons of the central nervous system and is activated by basal synaptic transmission, glutamate, and depolarization (Lilienbaum and Israel, 2003; Meffert and Baltimore, 2005). Whether it also non-transcriptionally regulates the functions of the central neurons remains elusive.

METHODS

All methods can be found in the accompanying Transparent Methods supplemental file.

SUPPLEMENTAL INFORMATION

Supplemental Information can be found online at https://doi.org/10.1016/j.isci.2019.08.017.

ACKNOWLEDGMENTS

The study was supported by National Natural Science Foundation of China (31771166 to X.-G.L; 81801112 to M.-X.X).

AUTHOR CONTRIBUTIONS

M.-X.X. performed the electrophysiology experiments, analyzed the data, and assisted in drafting the manuscript. X.-L.Z. performed western blot, co-immunoprecipitation, and microscopy and analyzed the data. J.X. performed western blot and behavioral tests and analyzed the data. D.L. performed microscopy. T.X. performed microscopy. W.-A.Z. and R.-P.P. analyzed the data. K.M. designed the experiments and helped to write the manuscript. X.-G.L. conceived the project, designed the experiments, and drafted the manuscript.

DECLARATION OF INTERESTS

The authors declare that they have no conflict of interests.

Received: March 12, 2019
Revised: July 4, 2019
Accepted: August 6, 2019
Published: September 27, 2019

REFERENCES

Aldrich, R.W., Corey, D.P., and Stevens, C.F. (1983). A reinterpretation of mammalian sodium channel gating based on single channel recording. Nature *306*, 436–441.

Campbell, T.M., Main, M.J., and Fitzgerald, E.M. (2013). Functional expression of the voltage-gated Na(+)-channel Nav1.7 is necessary for EGF-mediated invasion in human non-small cell lung cancer cells. J. Cell Sci. *126*, 4939–4949.

Catterall, W.A., Goldin, A.L., and Waxman, S.G. (2005). International Union of Pharmacology. XLVII. Nomenclature and structure-function relationships of voltage-gated sodium channels. Pharmacol. Rev. *57*, 397–409.

Chahine, M., and O'Leary, M.E. (2014). Regulation/modulation of sensory neuron sodium channels. Handb. Exp. Pharmacol. *221*, 111–135.

Chen, W., Sheng, J., Guo, J., Gao, F., Zhao, X., Dai, J., Wang, G., and Li, K. (2015). Tumor necrosis factor-alpha enhances voltage-gated Na(+) currents in primary culture of mouse cortical neurons. J. Neuroinflammation *12*, 126.

Cox, J.J., Reimann, F., Nicholas, A.K., Thornton, G., Roberts, E., Springell, K., Karbani, G., Jafri, H., Mannan, J., Raashid, Y., et al. (2006). An SCN9A channelopathy causes congenital inability to experience pain. Nature *444*, 894–898.

Dib-Hajj, S.D., Cummins, T.R., Black, J.A., and Waxman, S.G. (2007). From genes to pain: Nav1.7 and human pain disorders. Trends Neurosci. *30*, 555–563.

Dib-Hajj, S.D., Cummins, T.R., Black, J.A., and Waxman, S.G. (2010). Sodium channels in normal and pathological pain. Annu. Rev. Neurosci. *33*, 325–347.

Dresselhaus, E.C., Boersma, M.C.H., and Meffert, M.K. (2018). Targeting of NF-kappaB to dendritic spines is required for synaptic signaling and spine development. J. Neurosci. *38*, 4093–4103.

Fertleman, C.R., Baker, M.D., Parker, K.A., Moffatt, S., Elmslie, F.V., Abrahamsen, B., Ostman, J., Klugbauer, N., Wood, J.N., Gardiner, R.M., et al. (2006). SCN9A mutations in paroxysmal extreme pain disorder: allelic variants underlie distinct channel defects and phenotypes. Neuron *52*, 767–774.

Fujikawa, M., Nishitani, N., Ibuki, T., Kobayashi, S., and Matsumura, K. (2011). Sensory stimuli induce nuclear translocation and phosphorylation of nuclear factor kappa B in primary sensory neurons of mice. Neurosci. Res. *71*, 178–182.

Hayakawa, M., Miyashita, H., Sakamoto, I., Kitagawa, M., Tanaka, H., Yasuda, H., Karin, M., and Kikugawa, K. (2003). Evidence that reactive oxygen species do not mediate NF-kappaB activation. EMBO J. *22*, 3356–3366.

He, X.H., Zang, Y., Chen, X., Pang, R.P., Xu, J.T., Zhou, X., Wei, X.H., Li, Y.Y., Xin, W.J., Qin, Z.H., et al. (2010). TNF-alpha contributes to up-regulation of Nav1.3 and Nav1.8 in DRG neurons following motor fiber injury. Pain *151*, 266–279.

Heckscher, E.S., Fetter, R.D., Marek, K.W., Albin, S.D., and Davis, G.W. (2007). NF-kappaB, IkappaB, and IRAK control glutamate receptor density at the Drosophila NMJ. Neuron *55*, 859–873.

Huang, Y., Zang, Y., Zhou, L., Gui, W., Liu, X., and Zhong, Y. (2014). The role of TNF-alpha/NF-kappa B pathway on the up-regulation of voltage-gated sodium channel Nav1.7 in DRG neurons of rats with diabetic neuropathy. Neurochem. Int. *75*, 112–119.

Jarvis, M.F., Honore, P., Shieh, C.C., Chapman, M., Joshi, S., Zhang, X.F., Kort, M., Carroll, W., Marron, B., Atkinson, R., et al. (2007). A-803467, a potent and selective Nav1.8 sodium channel blocker, attenuates neuropathic and inflammatory pain in the rat. Proc. Natl. Acad. Sci. U S A. *104*, 8520–8525.

Jin, X., and Gereau, R.W., 4th (2006). Acute p38-mediated modulation of tetrodotoxin-resistant sodium channels in mouse sensory neurons by tumor necrosis factor-alpha. J. Neurosci. *26*, 246–255.

Kocmalova, M., Kollarik, M., Canning, B.J., Ru, F., Adam Herbstsomer, R., Meeker, S., Fonquerna, S., Aparici, M., Miralpeix, M., Chi, X.X., et al. (2017). Control of neurotransmission by NaV1.7 in human, Guinea pig, and mouse airway parasympathetic nerves. J. Pharmacol. Exp. Ther. *361*, 172–180.

Li, Y., North, R.Y., Rhines, L.D., Tatsui, C.E., Rao, G., Edwards, D.D., Cassidy, R.M., Harrison, D.S., Johansson, C.A., Zhang, H., et al. (2018). DRG voltage-gated sodium channel 1.7 is upregulated in paclitaxel-induced neuropathy in rats and in humans with neuropathic pain. J. Neurosci. *38*, 1124–1136.

Lilienbaum, A., and Israel, A. (2003). From calcium to NF-kappa B signaling pathways in neurons. Mol. Cell. Biol. *23*, 2680–2698.

Liu, B., Li, H., Brull, S.J., and Zhang, J.M. (2002). Increased sensitivity of sensory neurons to tumor necrosis factor alpha in rats with chronic compression of the lumbar ganglia. J. Neurophysiol. *88*, 1393–1399.

McCormack, K., Santos, S., Chapman, M.L., Krafte, D.S., Marron, B.E., West, C.W., Krambis, M.J., Antonio, B.M., Zellmer, S.G., Printzenhoff, D., et al. (2013). Voltage sensor interaction site for selective small molecule inhibitors of voltage-gated sodium channels. Proc. Natl. Acad. Sci. U S A *110*, E2724–E2732.

McDermott, L.A., Weir, G.A., Themistocleous, A.C., Segerdahl, A.R., Blesneac, I., Baskozos, G., Clark, A.J., Millar, V., Peck, L.J., Ebner, D., et al. (2019). Defining the functional role of NaV1.7 in human nociception. Neuron *101*, 905–919.e8.

Meffert, M.K., and Baltimore, D. (2005). Physiological functions for brain NF-kappaB. Trends Neurosci. *28*, 37–43.

Minett, M.S., Falk, S., Santana-Varela, S., Bogdanov, Y.D., Nassar, M.A., Heegaard, A.M., and Wood, J.N. (2014). Pain without nociceptors? Nav1.7-independent pain mechanisms. Cell Rep. *6*, 301–312.

Minett, M.S., Nassar, M.A., Clark, A.K., Passmore, G., Dickenson, A.H., Wang, F., Malcangio, M., and Wood, J.N. (2012). Distinct Nav1.7-dependent pain sensations require different sets of sensory and sympathetic neurons. Nat. Commun. *3*, 791.

Morinville, A., Fundin, B., Meury, L., Jureus, A., Sandberg, K., Krupp, J., Ahmad, S., and O'Donnell, D. (2007). Distribution of the voltage-gated sodium channel Na(v)1.7 in the rat: expression in the autonomic and endocrine systems. J. Comp. Neurol. *504*, 680–689.

Nassar, M.A., Stirling, L.C., Forlani, G., Baker, M.D., Matthews, E.A., Dickenson, A.H., and Wood, J.N. (2004). Nociceptor-specific gene deletion reveals a major role for Nav1.7 (PN1) in acute and inflammatory pain. Proc. Natl. Acad. Sci. U S A *101*, 12706–12711.

Niederberger, E., and Geisslinger, G. (2008). The IKK-NF-kappaB pathway: a source for novel molecular drug targets in pain therapy? FASEB J. *22*, 3432–3442.

Salles, A., Romano, A., and Freudenthal, R. (2014). Synaptic NF-kappa B pathway in neuronal plasticity and memory. J. Physiol. *108*, 256–262.

Schmalhofer, W.A., Calhoun, J., Burrows, R., Bailey, T., Kohler, M.G., Weinglass, A.B., Kaczorowski, G.J., Garcia, M.L., Koltzenburg, M., and Priest, B.T. (2008). ProTx-II, a selective inhibitor of NaV1.7 sodium channels, blocks action potential propagation in nociceptors. Mol. Pharmacol. *74*, 1476–1484.

Shields, S.D., Cheng, X., Uceyler, N., Sommer, C., Dib-Hajj, S.D., and Waxman, S.G. (2012). Sodium channel Na(v)1.7 is essential for lowering heat pain threshold after burn injury. J. Neurosci. *32*, 10819–10832.

Simpson, N.J., and Ferguson, A.V. (2017). The proinflammatory cytokine tumor necrosis factor-alpha excites subfornical organ neurons. J. Neurophysiol. *118*, 1532–1541.

Srinivasan, M., and Lahiri, D.K. (2015). Significance of NF-kappaB as a pivotal therapeutic target in the neurodegenerative pathologies of Alzheimer's disease and multiple sclerosis. Expert Opin. Ther. Targets *19*, 471–487.

Tamura, R., Nemoto, T., Maruta, T., Onizuka, S., Yanagita, T., Wada, A., Murakami, M., and Tsuneyoshi, I. (2014). Up-regulation of NaV1.7 sodium channels expression by tumor necrosis factor-alpha in cultured bovine adrenal chromaffin cells and rat dorsal root ganglion neurons. Anesth. Analg. *118*, 318–324.

Taniguchi, K., and Karin, M. (2018). NF-kappaB, inflammation, immunity and cancer: coming of age. Nat. Rev. Immunol. *18*, 309–324.

Wajant, H., and Scheurich, P. (2011). TNFR1-induced activation of the classical NF-kappaB pathway. FEBS J. *278*, 862–876.

Weiss, J., Pyrski, M., Jacobi, E., Bufe, B., Willnecker, V., Schick, B., Zizzari, P., Gossage, S.J., Greer, C.A., Leinders-Zufall, T., et al. (2011). Loss-of-function mutations in sodium channel Nav1.7 cause anosmia. Nature *472*, 186–190.

Xia, J., Huang, N., Huang, H., Sun, L., Dong, S., Su, J., Zhang, J., Wang, L., Lin, L., Shi, M., et al. (2016). Voltage-gated sodium channel Nav 1.7 promotes gastric cancer progression through MACC1-mediated upregulation of NHE1. Int. J. Cancer *139*, 2553–2569.

Zang, Y., He, X.H., Xin, W.J., Pang, R.P., Wei, X.H., Zhou, L.J., Li, Y.Y., and Liu, X.G. (2010). Inhibition of NF-kappaB prevents mechanical allodynia induced by spinal ventral root transection and suppresses the re-expression of Nav1.3 in DRG neurons in vivo and in vitro. Brain Res. *1363*, 151–158.

Zhang, J.M., Li, H., Liu, B., and Brull, S.J. (2002). Acute topical application of tumor necrosis factor alpha evokes protein kinase A-dependent responses in rat sensory neurons. J. Neurophysiol. *88*, 1387–1392.

Zsiros, E., Kis-Toth, K., Hajdu, P., Gaspar, R., Bielanska, J., Felipe, A., Rajnavolgyi, E., and Panyi, G. (2009). Developmental switch of the expression of ion channels in human dendritic cells. J. Immunol. *183*, 4483–4492.

ISCI, Volume *19*

Supplemental Information

Nuclear Factor-kappaB Gates $Na_v1.7$ Channels in DRG Neurons via Protein-Protein Interaction

Man-Xiu Xie, Xiao-Long Zhang, Jing Xu, Wei-An Zeng, Dai Li, Ting Xu, Rui-Ping Pang, Ke Ma, and Xian-Guo Liu

Supplemental Information

Figure. S1

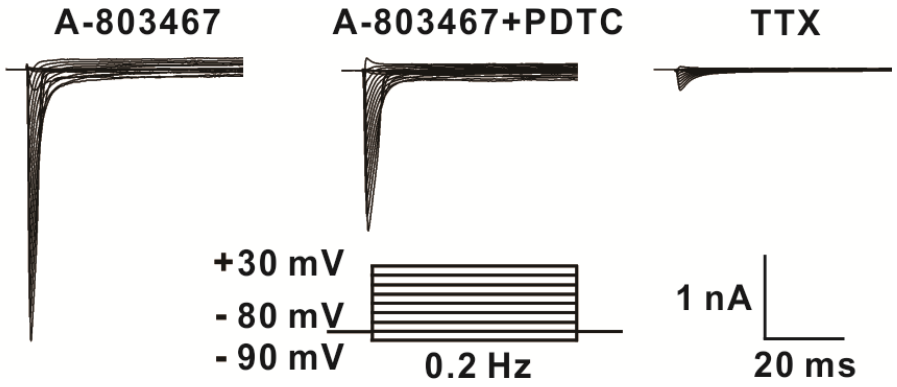

Figure S1. Isolation of TTX-S currents. Related to Figure 2. TTX-S currents were initially identified by their relatively fast activation and inactivation kinetics and recorded in the presence of TTX-R channel blocker A-803467 (1 μM). The identification was confirmed by adding 300 nM TTX at the end of the recordings. Only the current recordings that can be reduced by 90% or more with 300 nM TTX were used for further analysis.

Figure. S2

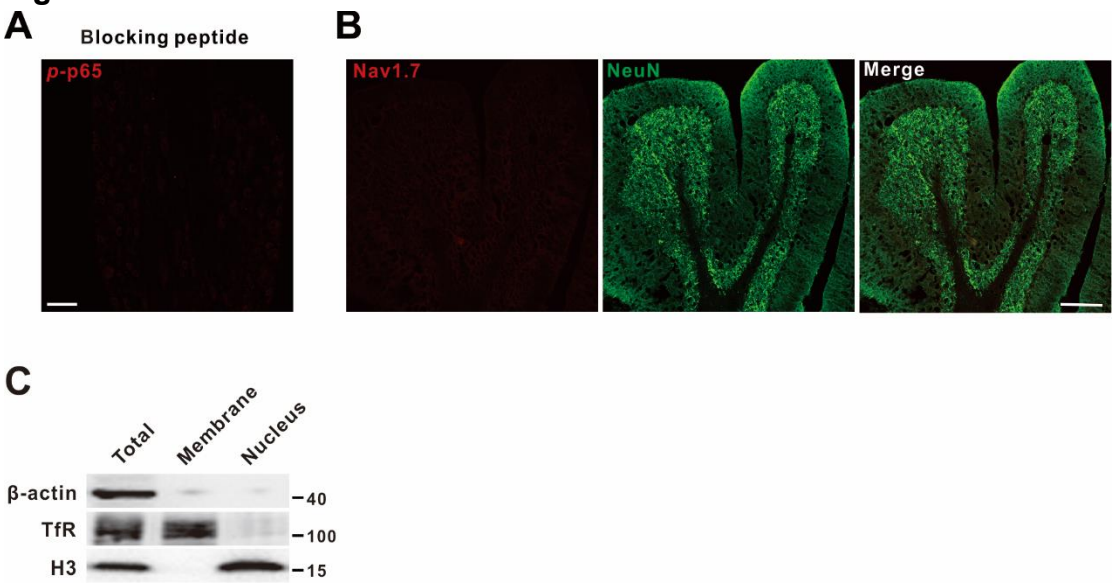

Figure S2. Identification of specificity of anti-*p*-p65 and anti-$Na_v1.7$, and the efficacy of extraction kit for isolation of membrane, cytoplasm and nuclear proteins used in this work. Related to Figure 1, Figure 3 and Figure 6. (A) The specificity of anti-*p*-p65 was identified by pre-incubation with *p*-p65 (s311) blocking peptides provided by manufacturer. Scale bars: 100 μm. (B) Anti-$Na_v1.7$ detect no signal in cerebellum which does not express $Na_v1.7$. Scale bars: 200 μm. (C) The expression of β-actin (marker of cytoplasmic protein), transferrin receptor (TfR) (marker of membrane protein) and histone H3 (marker of nucleoprotein) in the sample of total, membrane and nuclear extracts.

Transparent Methods

Animals

Male Sprague-Dawley rats (80 to 250 g) were purchased from the Institute of Experimental Animals of Sun Yat-sen University. The rats were individually housed in separate cages in a temperature-controlled (24 ± 1°C) and humidity-controlled (50-60%) room, under a 12/12-h light/dark cycle and with ad libitum access to sterile water and standard laboratory chow. All animal experimental procedures were approved by the local Animal Care Committee and were carried out in accordance with the guidelines of the National Institutes of Health on animal care and the ethical guidelines (Zimmermann, 1983). Animals were randomly assigned to different experimental or control conditions.

Preparation of pain models

Chemotherapy-induced peripheral neuropathy was induced by intraperitoneal injection of vincristine sulfate (0.1 mg/kg daily) for 10 consecutive days (Xu et al., 2017). Control animals received an equivalent volume of saline. Lumbar 5 spinal nerve ligation (L5-SNL) was done following the procedures described previously (Xie et al., 2017). Briefly, animals were anesthetized with halothane (2%), the left L5 spinal nerve was isolated adjacent to the vertebral column, and tightly ligated with a 6–0 silk sutures. While in sham-operated rat the L5 spinal nerve was identically exposed but not ligated.

Drug administration and behavioral test

Intrathecal injection of PDTC or vehicle was performed according to our previously described method (Zhang et al., 2018). In brief, a polyethylene-10 catheter was inserted into the rat's subarachnoid space through L5 and L6 intervertebral space and the tip of the catheter was located at the L5 spinal segmental level.

Mechanical sensitivity was assessed using von Frey hairs with the up-down method as described previously (Chaplan et al., 1994). Briefly, each rat was placed in a transparent Plexiglas testing chamber positioned on a wire mesh floor. A series of calibrated von Frey hairs with different bending forces were applied from below through the mesh floor to the sciatic innervation area of the hind paws for about 6-8 s with a 5 min interval between stimuli. Brisk withdrawal or licking of the paw in response to the stimulus was considered as positive response. The operator who performed the behavioral tests was blinded to all treatments.

DRG neuron preparation

Primary DRG neuron cultures were prepared from young Sprague-Dawley male rats (80~120 g body weight) as previously described (Xie et al., 2017; Zhang et al., 2018). In brief, L4-6 DRGs were freed from their connective tissue sheaths and broken into pieces with a pair of sclerotic scissors in DMEM/F12 medium (Gibco, USA) under low temperature. DRG neurons were plated on glass cover slips coated with Poly-L-Lysine (Sigma, USA) in a humidified atmosphere (5% CO_2, 37°C) following enzymatic and mechanical dissociation. The cells were used for electrophysiological recordings approximately 4 h to 24 h after plating.

Electrophysiology recordings

Whole-cell patch clamp recordings of Na^+ currents in DRG neurons were performed using an EPC-10 amplifier and the PULSE program (HEKA Electronics, Lambrecht, Germany) as

previously described (Xie et al., 2017). Currents were recorded with glass pipettes (3–5 MΩ resistance) fabricated from borosilicate glass capillaries using a Sutter P-97 puller (Sutter Instruments, Novato, CA). The currents were filtered at 10 kHz and sampled at 50 kHz. Voltage errors were minimized by using 80–90% series resistance compensation. The neurons with a leak current of > 500 pA or a series resistance of > 10 MOhm were excluded. For voltage clamp experiments, the extracellular solution contained (in mM): 30 NaCl, 20 TEA-Cl, 90 choline-Cl, 3 KCl, 1 $CaCl_2$, 1 $MgCl_2$, 10 HEPES, 10 glucose, and 0.1 $CdCl_2$ (adjusted to pH 7.3 with Tris base). The pipette solution contained (in mM): 135 CsF, 10 NaCl, 10 HEPES, 5 EGTA, and 2 Na_2ATP (adjusted to pH 7.2 with CsOH). For recording TTX-S currents 1 μM A-803467 was included to block the TTX-R Na^+ currents. TTX-S Na^+ currents were identified initially by their relatively fast activation and inactivation kinetics and was confirmed by adding 300 nM TTX at the end of the recordings. Only the current recordings that can be reduced by 90% or more with 300 nM TTX were used for further analysis (Figure S1). And for recording TTX-R Na^+ currents 300 nM TTX was included to block the TTX-S channels (Tanaka et al., 2015). $Na_v1.7$ current was isolated from total Na^+ currents by subtraction of the ProTxII-resistant Na^+ currents from total current using a previously published subtraction protocol (Li et al., 2018; Schmalhofer et al., 2008). In this work, we randomly recorded 153 neurons, including 33 large size of neurons (> 35 μm), 84 medium size of neurons (25-35 μm) and 36 small size of neurons (< 25 μm).

To study the effects of different chemicals on Na_v channels, Na^+ current was elicited by a depolarization potential (from -90 mV to -10 mV, 100 ms). The amplitude of currents evoked by the *n*th impulse was normalized to the current evoked by the first impulse. For calculation of I-V curves, Na^+ current was evoked from a holding potential of -90 mV and then depolarized from -80 mV to +60 mV at 5 mV steps. Current density was calculated by normalizing maximal peak currents with cell capacitance.

To investigate the mechanisms by which *p*-p65 may regulate $Na_v1.7$ channels, The effects of PDTC on activation, inactivation and recovery of $Na_v1.7$ channels were determined in HEK293 cells that express Nav1.7. For building activation curves, the cell was clamped at a holding potential of -90 mV and a prepulse voltage to -120 mV for 200 ms was applied. $Na_v1.7$ current was elicited by a stepped depolarization test voltage pulse from -80 mV to 100 mV for 50 ms. To build steady state fast inactivation curves, the cell was clamped at a holding potential of -90 mV, a stepped prepulse from -120 mV to 40 mV with 5 mV increments for 1000 ms was applied, and the $Na_v1.7$ current was recorded at a voltage of 0 mV. Time constants for recovery from the inactivation of $Na_v1.7$ channel was measured with a double-pulse protocol. A first pulse (P1) for 250 ms to -10 mV caused inactivation, and $Na_v1.7$ current evoked by the test pulse (P2) to -10 mV after variable intervals was compared with $I_{Na,P1}$ of the same episode.

The activation or inactivation conductance variables of I_{Na} were determined with normalized currents. Current activation and inactivation were fitted by the Boltzmann distribution: $y=1/\{1+\exp[(V_m-V_{0.5})/S]$, where V_m is the membrane potential, $V_{0.5}$ is the activation or inactivation voltage mid-point, and S is the slope factor. The relation of $1/\tau_{block}$ against the concentration is described by the linear function: $1/\tau_{block}=k[D]+l$, where $1/\tau_{block}$ is the time constant of development of block, and k and l are the apparent rate constants for association and dissociation of the drug.

Western blot

The L4-6 DRGs were dissected and homogenized in cold RIPA buffer [50 mM Tris-HCl (pH 7.4), 150 mM NaCl, 0.1% Triton X-100, 1% sodium deoxycholate, 0.1% SDS, 10 mM NaF, 1 mM EDTA, 1 mM PMSF, and 1 mg/ml leupeptin]. Membrane, cytoplasm and nuclear proteins were isolated with the protein extraction kit (Invent Biotechnologies, SM-005). The isolation efficacy of the kit was identified (Figure S2C). The protein samples were separated via gel electrophoresis (SDS-PAGE) and transferred onto a PVDF membrane. The membranes were placed in blocking buffer for 1 h at room temperature and incubated in a primary antibody against *p*-p65 (ser311) (1:100, mouse; Santa Cruz Biotechnology; sc-135769), transferrin receptor (TfR) (1:1000, mouse; Invitrogen; QG215340), $Na_v1.3$, $Na_v1.6$, $Na_v1.7$, $Na_v1.8$, $Na_v1.9$ (1:200, rabbit; Alomone Labs; ASC-004 for $Na_v1.3$; ASC-009 for $Na_v1.6$; ASC-008 for $Na_v1.7$; ASC-016 for $Na_v1.8$; ASC-017 for $Na_v1.9$), Histone H3 (1:1000, rabbit; Affinity; AF0863) overnight at 4°C. And then, the membranes were incubated in HRP-conjugated secondary antibody. Enhanced chemiluminescence (ECL) solution (Milipore) was used to detect the immunocomplexes. Each band was quantified with a computer-assisted imaging analysis system (Tanon Gis).

Co-Immunoprecipitation

The dissected DRG tissues were lysed in cold co-IP RIPA buffer [20 mM Tris-HCl (pH 7.5), 150 mM NaCl, 0.1% Triton X-100, 1% sodium deoxycholate, 10 mM NaF, 1 mM EDTA, 1 mM PMSF, and 1 mg/ml leupeptin]. The lysate was centrifuged and 5% of the supernatant was used for input sample. The remaining supernatant was precipitated with 10 μg anti-*p*-p65 or anti-$Na_v1.7$ at 4°C overnight and then with protein A/G beads (GE Healthcare) at 4°C for 4 h. The immunoprecipitated sample was denatured and prepared for immunoblotting. Immunoprecipitation was performed with antibodies against $Na_v1.3$, $Na_v1.6$, $Na_v1.7$, $Na_v1.8$, $Na_v1.9$ and *p*-p65.

Immunohistochemistry and structured illumination microscopy

Rats were perfused with 4% paraformaldehyde (PFA). The L4-6 DRGs were dissected and post-fixed in 4% PFA for 1 h. Then the tissues were dehydrated in 30% sucrose and embedded for cryostat sectioning. The cryostat sections were incubated with primary antibodies against *p*-p65 (ser311) (1:50, rabbit; Santa Cruz Biotechnology; sc-33039), $Na_v1.7$ (1:100, mouse; Abcam; ab85015), IB4 (1:50; Sigma; L2895), CGRP (1:200, mouse; Abcam; ab81887), NF200 (1:200, mouse; Sigma; N0142), GFAP (1:400, mouse; Cell signaling technology; 3670) at 4°C overnight, and then incubated in secondary antibodies for 1 h at room temperature. Three-dimensional super-resolution images were captured using a three-dimensional structured illumination microscope with the N-SIM System and an oil immersion objective lens CFI SR (Apochromat TIRF×100, 1.49 numerical aperture, Nikon, Japan), and images were post-processed with Nikon NIS-Elements software. The specificity of the antibody for *p*-p65 (s311) and $Na_v1.7$ was identified in Figures S2A and S2B.

Solutions and chemicals

All solution was adjusted to pH 7.35-7.40 and to osmolality 310 mOsm. Vincristine sulfate (Main Luck Pharmaceuticals Inc.) was dissolved in saline to a concentration of 50 μg/ml immediately before application. Tetrodotoxin (Absin) was dissolved as a stock of 1 mM in acetic acid aqueous solution and diluted to a working concentration of 300 nM. A-803467 (Selleck) was dissolved in DMSO as a stock of 1 mM, diluted to 1 μM with extracellular solution. TNF-α (R&D) were dissolved with in sterile PBS containing 0.1% bovine serum albumin and diluted to work concentration (100 nM). ProTxII (TOCRIS) were dissolved with distilled water and diluted

to work concentration (5 nM) with extracellular solution. ICA121431 (MCE) was dissolved with distilled water and diluted to work concentration (5 μM) with extracellular solution. PDTC (Sigma Aldrich) was diluted to 10 nM in extracellular solution. *P*-p65 antibody (rabbit; Santa Cruz Biotechnology) was diluted to 10 μg/ml in pipette solution.

Data analysis

All data were expressed as mean ± SD, and analyzed with GraphPad Prism 7. Threshold for statistical significance was $P < 0.05$. Although no power analysis was performed, the sample size was determined according to previous publications in pain-associated behavior and molecular studies.

References

Chaplan, S.R., Bach, F.W., Pogrel, J.W., Chung, J.M., and Yaksh, T.L. (1994). Quantitative assessment of tactile allodynia in the rat paw. J Neurosci Methods *53*, 55-63.

Tanaka, K., Sekino, S., Ikegami, M., Ikeda, H., and Kamei, J. (2015). Antihyperalgesic effects of ProTx-II, a Nav1.7 antagonist, and A803467, a Nav1.8 antagonist, in diabetic mice. Journal of experimental pharmacology *7*, 11-16.

Xie, M.X., Pang, R.P., Yang, J., Shen, K.F., Xu, J., Zhong, X.X., Wang, S.K., Zhang, X.L., Liu, Y.Q., and Liu, X.G. (2017). Bulleyaconitine A preferably reduces tetrodotoxin-sensitive sodium current in uninjured dorsal root ganglion neurons of neuropathic rats probably via inhibition of protein kinase C. Pain *158*, 2169-2180.

Xu, T., Li, D., Zhou, X., Ouyang, H.D., Zhou, L.J., Zhou, H., Zhang, H.M., Wei, X.H., Liu, G., and Liu, X.G. (2017). Oral Application of Magnesium-L-Threonate Attenuates Vincristine-induced Allodynia and Hyperalgesia by Normalization of Tumor Necrosis Factor-alpha/Nuclear Factor-kappaB Signaling. Anesthesiology *126*, 1151-1168.

Zhang, X.L., Ding, H.H., Xu, T., Liu, M., Ma, C., Wu, S.L., Wei, J.Y., Liu, C.C., Zhang, S.B., and Xin, W.J. (2018). Palmitoylation of delta-catenin promotes kinesin-mediated membrane trafficking of Nav1.6 in sensory neurons to promote neuropathic pain. Science signaling *11*.

Zimmermann, M. (1983). Ethical guidelines for investigations of experimental pain in conscious animals. Pain *16*, 109-110.